Stem Cell Rev and Rep
DOI 10.1007/s12015-016-9669-1

Non-Washed Resorbable Blasting Media (NWRBM) on Titanium Surfaces could Enhance Osteogenic Properties of MSCs through Increase of miRNA-196a And VCAM1

Chiara Gardin[1] · **Letizia Ferroni**[1] · **Adriano Piattelli**[2] · **Stefano SIvolella**[3] · **Barbara Zavan**[1] · **Eitan Mijiritsky**[4]

© Springer Science+Business Media New York 2016

Abstract Surface topography of Titanium (Ti) dental implants strongly influences osseointegration. In the present work, we have analyzed the influence of two Ti implant surfaces characterized by similar microtopography but different nanotopography and chemistry on the osteoblastic phenotype of Dental Pulp Stem Cells (DPSCs). The effect on osteogenic differentiation, extracellular matrix (ECM) and cell adhesion molecules production have been evaluated by means of molecular biology analyses. The morphology of the cells grown onto these surfaces has been analyzed with SEM and immunofluorescence (IF), and the safety of the surfaces has been tested by using karyotype analysis, Ames test and hemocompatibility assay. Results showed that starting from 15 days of DPSCs culture, a substantial expression of osteoblast specific markers and a strong increase of cell adhesion molecules can be detected. In particular, when DPSCs are seeded on the Ti implants expression of microRNA (miRNA)-196a, which is involved in osteoblastic commitment of stem cells, and of Vascular Cell Adhesion Molecule 1 (VCAM1), a factor involved in angiogenesis, is strongly enhanced.

✉ Barbara Zavan
barbara.zavan@unipd.it

[1] Department of Biomedical Sciences, University of Padova, Via U. Bassi 58/B, 35131 Padova, Italy

[2] Department of Stomatology and Biotechnologies, University of Chieti-Pescara, Chieti, Italy

[3] Department of Neurological Sciences, University of Padova, Via U. Bassi 58/B, 35131 Padova, Italy

[4] Department of Oral Rehabilitation, School of Dental Medicine, Tel-Aviv University, Ramat Aviv, Israel

Published online: 18 June 2016

Keywords Stem cells · Titanium · Dental implant; osseointegration ; surfaces · Nanotopography · Titanium implants

Introduction

In 1977, Brånemark and coworkers published a paper entitled "Osseointegrated implants in the treatment of the edentulous jaw. Experience from a 10-year period". In this study, the authors demonstrated that it was possible to replace lost teeth by means of Titanium (Ti)-based implants. This technique has revolutionized clinical dentistry and today is a routine procedure mostly standardized. [1, 2] It requires the preparation of the recipient bone site with drills; then, the Ti screw is placed at defined torque and speed. Following these operations, few months are needed before insertion of a definitive restoration. A key factor to obtain good osseointegration is represented by the time. [3, 4] At a biological level, osseointegration is defined as close contact between the implant surface and the surrounding bone. [5, 6] This is strictly dependent on the surface geometry and topography of the device. For this reason, several researches have put great attention in dental implant technology. Many studies have struggled to enhance the osseointegrative properties of implants by various surface modifications [7–10].

It is well known that external stimuli are able to influence stem cell fate through several ways regulating in the end cell shape. [11] Cell shape is a powerful regulator of cell physiology, and stem cell destiny can be influenced by artificially controlling ExtraCellular Matrix (ECM) composition. [12–15] Indeed, in vitro modulation of topographical features influences cell functions likewise to that provided by the ECM geometry in vivo. [16, 17] In addition, topographic surfaces with nanoscale features are able to induce changes in cell

polarization, elongation, migration, proliferation, and gene expression. [18–20] Topographical cues might be used as a tool to induce stem cell differentiation into different cell types for the validation of nanostructured scaffolds [21–23]..

Surface modifications directed at altering both chemistry and topography of the implants for the improvement of osseointegration have been the focus of several investigations. [24–27] Recently, the use of Resorbable-Blasting Media (RBM) has shown interesting results. [28] In their work, Bonfante et al. evidenced that the use of additional treatment to RBM surfaces without subsequent acid-etching, Non-Washed RBM (NWRBM), strongly improves the osseointegration process. The results obtained in this study are promising and suggest further investigation relating to NWRBM's interaction with stem cell.

In this work, we aimed at studying the biological events related to the osseointegration process, focusing in particular on the early interactions between human Dental Pulp Stem Cells (DPSCs) and Ti dental implants surfaces. The behavior of DPSCs seeded on two different Ti surfaces with similar microtopography but different nanotopography and chemistry has been evaluated and compared in terms of biocompatibility and osteogenic differentiation of stem cells.

Material and Methods

Ti Dental Implants

In this in vitro study, two types of Ti dental implants (10 mm long and 3.75 mm in diameter; Adin Dental Implant Systems Ltd., Afula, Israel) with similar microtopography but different nanotopography and chemistry were used: OsseoFix Non-Washed Resorbable Blasting Media (NWRBM) as experimental implants, and Alumina-Blasted/Acid-Etched (AB/AE) as control implants. All dental implants were sterilized by γ-rays.

Hemolysis Assay

The hemolysis assay was performed following standard practices set forth in ASTM F756 for evaluating the blood compatibility of the experimental and control Ti implants, as reported in Gardin et al. [29] Blood of three healthy New Zealand rabbits was pooled and diluted in Phosphate Buffer Saline (PBS; Lonza S.r.l., Milano, Italy) to achieve a total hemoglobin concentration of 10 ± 1 mg/mL. One mL of this blood was added to 7 mL of the following PBS extracts: triplicate 2 g portions of Ti experimental or control implants in 10 mL PBS (test materials); triplicate 30 cm [2] portions of High Density PolyEthylene (HDPE) in 10 mL of PBS (negative control); triplicate 10 mL portions of Sterile Water for Injection (SWFI) (positive control). Extraction conditions were 50 °C for 72 h. Each sample was incubated for 3 h at 37 °C, then centrifuged for 15 min at 800 g. One mL of the resulting supernatant from all samples was added to 1 mL of Drabkin's reagent (Sigma-Aldrich, St. Louis, MO, USA) and incubated at room temperature for 15 min. The reaction product was quantified with a multilabel plate reader (Victor 3, Perkin Elmer, Milano, Italy) by measuring Optical Density (OD) at 540 nm. The hemolysis index (HI) was then calculated using the mean OD for each group as follows:

$$HI(\%) = OD(\text{test material}) - OD(\text{negative control}) / OD(\text{positive control}) - OD(\text{negative control}) \times 100.$$

For HI ≤ 2 %, the sample is considered nonhemolytic; for HI > 2 %, the sample is considered hemolytic.

Ames Test

The mutagenic potential of experimental and control Ti implants was evaluated with the Ames test by using the Salmonella Mutagenicity Complete Test Kit (Moltox, Molecular toxicology Inc., Boone, NC, USA), as described in Ferroni et al. [30] Briefly, Ti implants were extracted for (24 ± 2) h at (37 ± 1) °C, using nutrient broth (blank) as the extraction vehicle. The same extraction conditions were set for Aluminium oxide ceramic rod (VITA In-Ceram Alumina CA-12, CE 0124, lot 15,320) (negative control), and ICR 191 Acridine (Moltox, 60–101) and Sodium Azide (Moltox, 60–103) (positive controls). Four different strains of Salmonella were incubated for 48 h at 37 °C with the different extracts; then, the number of revertant colonies per plate was counted. Three replicates were performed for each sample. If the number of reverted colonies is equivalent to those observed with blank and negative control, the sample is considered not mutagenic; if the number of reverted colonies is equivalent to those observed with positive controls, the sample is considered mutagenic.

Cell Isolation and Seeding onto Ti Implants

Human DPSCs isolation was performed as described in Bressan et al. [31] Briefly, human dental pulps were extracted from healthy molar teeth of subjects, who had given written consent, by means of a dentinal excavator or a Gracey curette after mechanical fracturing. The removed pulp was digested in a solution of 3 mg/mL type I collagenase and 4 mg/mL dispase in PBS for 1 h at 37 °C. The isolated cells were then cultured in complete DMEM (cDMEM) made of Dulbecco's Modified Eagle Medium (DMEM) (Lonza S.r.l. Milano, Italy), 10 % Fetal Bovine Serum (FBS; Bidachem S.p.A., Milano, Italy), 100 U/mL penicillin and 100 U/mL streptomycin (Lonza S.r.l). At confluence, cells were detached from culture plates with trypsin (Lonza S.r.l), then seeded onto the experimental and control Ti implants at a density of 1x10 [6] cells/implant in 6-well plates. The cells were cultured in

Table 1 Human primer sequences

gene symbol	forward primer (5′ → 3′)	reverse primer (5′ → 3′)
COL1A1	TGAGCCAGCAGATCGAGA	ACCAGTCTCCATGTTGCAGA
GAPDH	TCAACAGCGACACCCAC	GGGTCTCTCTCTTCCTCTTGTG
OCN	GCAGCGAGGTAGTGAAGAGAC	AGCAGAGCGACACCCTA
ON	TGCATGTGTCTTAGTCTTAGTCACC	GCTAACTTAGTGCTTACAGGAACCA
OPN	TGGAAAGCGAGGAGTTGAATGG	GCTCATTGCTCTCATCATTGGC
RUNX2	AGCCTTACCAAACAACACAACAG	CCATATGTCCTCTCAGCTCAGC

Abbreviations: *COL1A1* collagen, type I, alpha 1; *GAPDH* glyceraldehyde-3-phosphate dehydrogenase; *OCN* osteocalcin; *ON* osteonectin; *OPN* osteopontin; *RUNX2* runt-related transcription factor 2

cDMEM at 37 °C with 5 % CO_2 up to 30 days, changing the medium every two days.

MTT Assay

The viability of DPSCs seeded onto experimental and control Ti implants was evaluated at 1, 3, 15 and 30 days of culture using the Methyl Thiazolyl-Tetrazolium (MTT)-based cytotoxicity assay, as described in Denizot and Lang with minor modifications. [32] The samples were incubated in 1 mL of 0.5 mg/mL MTT solution in PBS for 3 h at 37 °C. After removing the MTT solution, each sample was extracted with 0.5 mL of 10 % dimethyl sulfoxide in isopropanol (iDMSO) for 30 min at 37 °C. For each sample, 200 μL aliquots in duplicate were used for OD recordings at 570 nm by means of a multilabel plate reader (Victor 3).

Scanning Electron Microscopy (*SEM*)

For SEM imaging, DPSCs grown on experimental and control Ti implants for 30 days were fixed in 2.5 % glutaraldehyde in 0.1 M cacodylate buffer for 1 h, then progressively dehydrated in ethanol. The SEM analysis was carried out at the Interdepartmental Service Center C.U.G.A.S. (University of Padova, Italy).

Table 2 miRNA regulating the osteogenic and adipogenic differentiation of MSCs

miRNA	Target gene	Effect
mir-26a	SMAD1	Suppress osteogenesis
mir-100	BMPR2	Suppress osteogenesis
mir-31	BMPR2	Suppress osteogenesis
mir-106a	BMPR2	Suppress osteogenesis
mir-486-5p	SIRT1	Suppress osteogenesis
mir-196a	HOXC8	Promote osteogenesis
mir-218	SFRP2, DKK3	Promote osteogenesis
mir-22	HDAC6	Promote osteogenesis
mir-148	RUNX2, OCN	Promote osteogenesis

Abbreviations: *SMAD1* SMAD family member 1; *BMPR2* bone morphogenetic protein receptor type II; *SIRT1* sirtuin 1; *HOXC8* homeobox C8; *SFRP2* secreted frizzled-related protein 2; *DKK3* dickkopf WNT signaling pathway inhibitor 3; *HDAC6* histone deacetylase 6; *RUNX2* runt related transcription factor 2; *OCN* osteocalcin

Karyotype Analysis

DPSCs seeded onto experimental Ti implants for 30 days were subjected to karyotype analysis by capturing the metaphases by colchicine (Sigma-Aldrich) exposure for 6 h. Metaphases of cells were stained by the Q-banding technique and karyotyped according to the International System for Human Cytogenetic Nomenclature. Twenty-five metaphases were analyzed for three expansions.

Total RNA and miRNA Isolation

Total RNA including microRNAs (miRNAs) were isolated with miRNeasy Mini Kit (Qiagen GmbH, Hilden, Germany) from DPSCs seeded onto experimental and control Ti implants after 15 and 30 days of culture. NanoDropTM ND-1000 (Thermo Fisher Scientific, Waltham, MA, USA) was used to assess quality and concentration of the RNA samples.

Real-Time PCR

Complementary DNA (cDNA) was made from 200 ng of total RNA using M-MLV Reverse Transcriptase (Invitrogen, Carlsbad, CA, USA) or miRcute miRNA First-strand cDNA Synthesis Kit (Tiangen Biotech, Shangai, China), following the manufacturer's protocols. Human primer sequences are detailed in Table 1. Real-time PCRs were performed with a Rotor-Gene 3000 (Corbett Research, Sydney, Australia) using 300 nM concentration of the designed primers and FastStart SYBR Green Master (Roche Diagnostics, Mannheim, Germany). Differences in gene expression were evaluated by the 2ΔΔCt method, [33] using DPSCs seeded onto control Ti implants as control condition. Values were normalized to the expression of the Glyceraldehyde-3-Phosphate

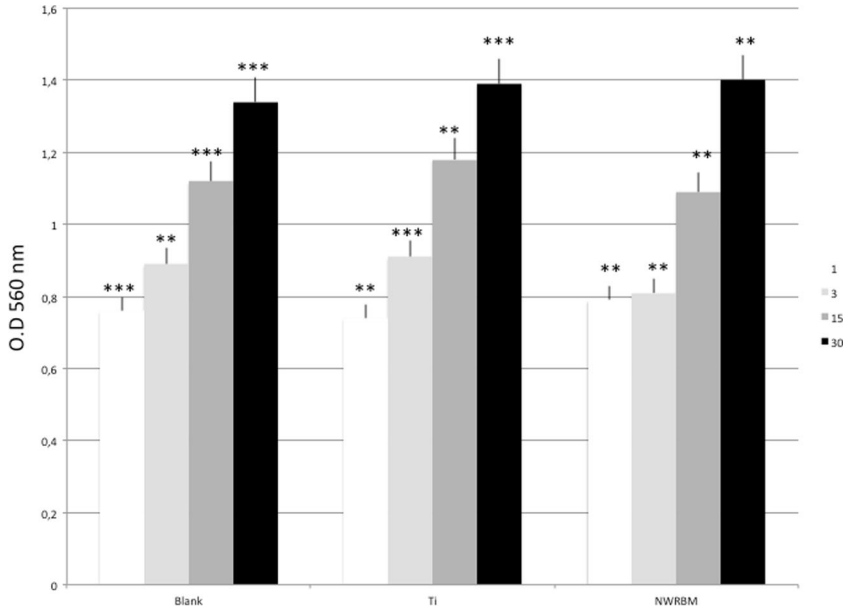

Fig. 1 Biocompatibility of Ti implants
Notes: The viability of DPSCs seeded onto experimental and control implants was measured with the MTT assay at 1, 3, 15, and 30 days of culture. Cells cultured in plastic culture dish were used as control. Data are given as the mean ± standard deviation ($n = 3$ per group).

DeHydrogenase (GAPDH) housekeeping gene. The mature miRNAs (Table 2) expression levels in DPSCs seeded onto experimental and control implants were estimated with the miRcute miRNA qPCR detection kit (Tiangen). The relative miRNA levels were calculated by the 2ΔCt method after normalization to snRNA-U6 expression.

RT [2] Profiler PCR Array

For the first-strand cDNA synthesis, 200 ng of total RNA of each sample was reverse transcribed with the RT [2] First Strand kit (Qiagen). Real-time PCR was performed according to the user manual of the Human Extracellular Matrix & Adhesion Molecules RT [2] Profiler PCR array (SABiosciences, Frederick, MD, USA) using RT [2] SYBR Green ROX FAST Mastermix (SABiosciences). This array profiles the expression of genes important for cell-cell and cell-matrix interactions. Real-time PCRs were carried out on a Rotor-Gene Q 100 (Qiagen). Data were analyzed using Excel-based PCR Array Data Analysis templates (SABiosciences). Results were given as the mRNA relative expression of each target gene in DPSCs seeded on experimental implants compared to control implants.

Immunofluorescence (IF)

DPSCs seeded on the experimental Ti implants for 30 days were fixed in 4 % paraformaldehyde (Sigma-Aldrich) in PBS for 30 min, then incubated in 2 % Bovine Serum Albumin (BSA, Sigma-Aldrich) solution in PBS for 30 min at room temperature. The implants were then incubated with the rabbit anti-human osteopontin (Abcam, Cambridge, UK) primary antibody in 2 % BSA overnight at 4 °C. IF staining was performed with the secondary antibody anti-rabbit IgG DyLight 488 labeled (KPL, Gaithersburg, MD, USA) in 2 % BSA for 1 h at room temperature. Nuclear staining was made with 2 mg/mL Hoechst H33342 (Sigma-Aldrich) solution for 5 min. All images were obtained using a Leica DMI4000 (Leica Microsystems GmbH, Wetzlar, Germany).

Alkaline Phosphatase (ALP) activity measurements

The intracellular and extracellular ALP activity of DPSCs seeded onto the experimental and control Ti implants for 30 days were measured using Alkaline Phosphatase Assay kit (colorimetric) (Abcam). According to the manufacturer protocol, the culture medium from each sample group was collected and pooled together. At the same time, cells on implants were washed with PBS, homogenized with ALP Assay

Table 3 Results of the hemolysis assay

sample	OD	Hemolysis index	results
Positive control	0.8954 ± 0.013	100 %	Hemolytic
Negative control	0.0148 ± 0.002	0 %	Nonhemolytic
Experimental implant	0.0151 ± 0.002	0.034 %	Nonhemolytic
Control implant	0.0154 ± 0.002	0.068 %	Nonhemolytic

Table 4 Results of the Ames test

	STDisc™ TA1535		STDisc™ TA1537		STDisc™ TA98		STDisc™ TA100	
sample	revertant colonies	mutagenic	revertant colonies	mutagenic	revertant colonies	mutagenic	revertant colonies	mutagenic
blank	4 ± 3	no	5 ± 3	no	5 ± 3	no	3 ± 3	no
Negative control	3 ± 2	no	4 ± 2	no	2 ± 2	no	4 ± 2	no
Positive control: ICR191	922 ± 76	yes	928 ± 76	yes	921 ± 76	yes	929 ± 76	yes
Positive control: Sodium Azide	847 ± 50	yes	851 ± 50	yes	844 ± 50	yes	849 ± 50	yes
Experimental implant	3 ± 2	no	4 ± 2	no	2 ± 2	no	4 ± 2	no
Control implant	4 ± 2	no	2 ± 2	no	3 ± 2	no	4 ± 2	no

Buffer (300 μL in total for each group), then centrifuged at 13,000 rpm for 3 min to remove insoluble material. Different volumes of samples (medium and cells) were then added into 96-well plate, bringing the total volume in each well up to 80 μL with Assay Buffer. 80 μL of fresh medium was also used as sample background control. Thereafter, 50 μL of 5 mM p-nitrophenyl phosphate (pNPP) substrate solution was added to each well containing test samples and background control and incubated for 60 min at 25 °C, protecting the plate from the light. A standard curve of 0, 4, 6, 12, 16, and 20 nmol/well was generated from 1 mM pNPP standard solution bringing the final volume to 120 μL with Assay Buffer. OD values were recorded at 405 nm in a microplate reader (Victor 3), after stopping all reactions, except the sample background control, with 20 μL of Stop solution. The results were normalized subtracting the value derived from the zero standards from all standards, samples and sample background control. The pNP standard curve was plotted to identify the pNP concentration in each sample. ALP activity of the test samples was calculated as follows:

$$\text{ALP activity}\left(\text{U}/\text{mL}\right) = \text{A}/\text{V}/\text{T}$$

where A is the amount of pNP generated by samples (in μmol), V is the amount of sample added in the assay well (in mL), and T is the reaction times (in minutes).

Statistical Analysis

Statistical analysis was performed using SPSS software (SPSS Inc., Chicago, IL, USA). The mean values for quantitative data were compared applying non-parametric Kruskal–Wallis test for Real time PCR results. Parametric one-way ANOVA analysis was applied for MTT, hemolysis assay, Ames test and ALP activity data, following by a post-hoc Tukey test. p values ≤0.05 were considered statistically significant.

Results and Discussion

Biocompatibility of the Ti Implants

When a material has to be employed in a living organism, excellent biocompatibility is fundamental in order to prevent any adverse effect. The biocompatibility of experimental and control Ti implants has been evaluated by measuring the viability of DPSCs seeded onto the implants up to 30 days with the MTT assay (Fig. 1). Cells cultured on plastic culture dish were used as control. The OD values recorded for cells loaded on Ti implants were found to be very similar to those observed for the control, thus indicating that DPSCs are able to grow well on both the tested implants. The blood compatibility of the experimental and control Ti implants has been tested with the hemolysis assay. This is of particular importance since dental implants are intended for blood contacting applications. The test quantifies free hemoglobin released into the plasma following blood cells damage. As reported in Table 3, no hemoglobin has been detected demonstrating the lack of any hemolytic activity of both the Ti implants. At the same time, the mutagenic potential of the dental implants has been excluded by performing the Ames test. As reported in Table 4, a negative result indicates that the tested materials are not

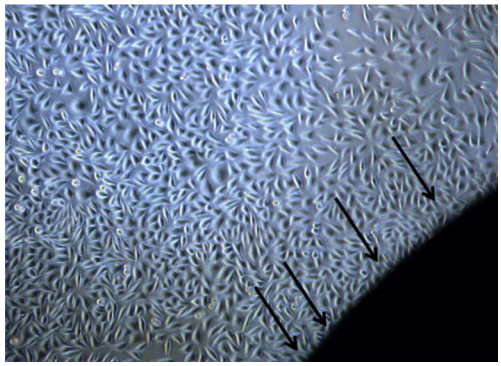

Fig. 2 Morphological analysis of DPSCs grown on Ti implants
Notes: SEM images of DPSCs seeded for 30 days in cDMEM onto (A) experimental and (B) control implant (500X magnification).

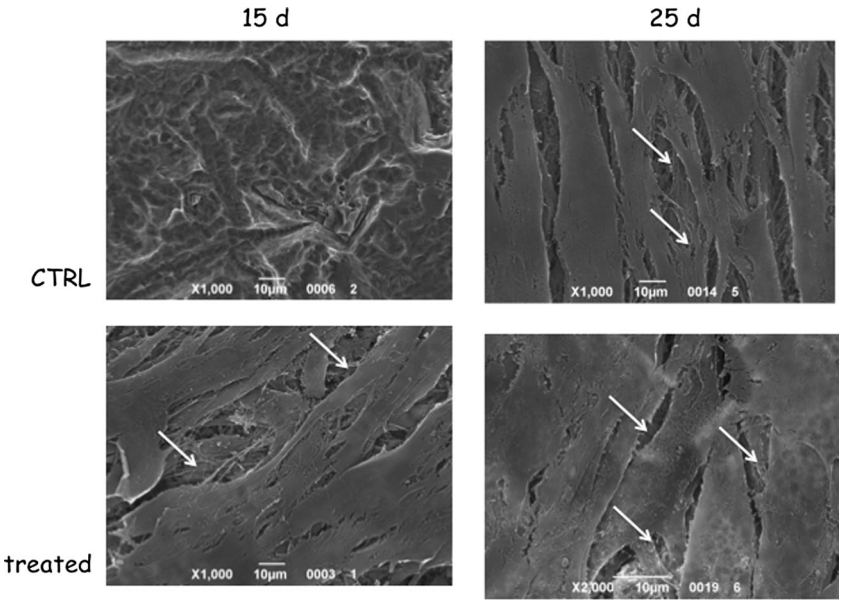

Fig. 3 Karyotype analysis
Notes: Karyotype of DPSCs seeded onto experimental implant for 30 days showing no chromosomal abnormalities.

mutagenic and therefore may not act as a carcinogen, since cancer is often linked to mutations.

Electron microscopy performed at SEM evidenced that DPSCs adhering to the implant surfaces assumed a typical osteoblastic morphology at day 30 (Fig. 2). Images also showed that cells were flat and overlapped on both the surfaces, thus favoring communication with each other. From SEM images it was also possible to observe that cells developed long filopodia. Nevertheless, cells cultured onto experimental implants were characterized by larger size compared to cells seeded on the control ones. These observations were confirmed by measurements with Image J software, indicating that the area of the cells cultured for 30 days on experimental implants was approximately four times higher (12.25 μm [2]) than that cultured on control (3.02 μm [2]).

The biological safety of NWRBM implants has been established by performing karyotype analysis of DPSCs after 30 days of culture on these implants. Karyotyping evaluates the presence of chromosomes unbalances due to amplification and differentiation of the cells on the surface of the implants. DPSCs did not show any chromosomal alteration, thus indicating the genomic stability of the cells during long term cultures on experimental Ti implants (Fig. 3).

Effect of Ti Implants on Osteogenic Differentiation of DPSCs

In order to test if the Ti implants possess osteogenic properties, the expression of the principal osteogenic markers in DPSCs cultured for 15 and 30 days on the implants has been evaluated. Among the osteogenic markers, we investigated the expression of COL1A1, the protein representing the 90 % of the bone protein mass; ON, an ECM protein that in association with COL1A1 induces mineral deposition; OPN, an extracellular structural protein which expression in bone predominantly occurs by osteoblasts and osteocytes; OCN, another noncollagenous protein found in bone and secreted solely by osteoblasts; and RUNX2, the early bone Transcription Factor (TF). Figure 4 shows mRNA relative expression levels of these genes. From the histograms, it is evident an increase of the mRNAs encoding for these molecules over time, and this increase is more evident in DPSCs cultured onto the NWRBM

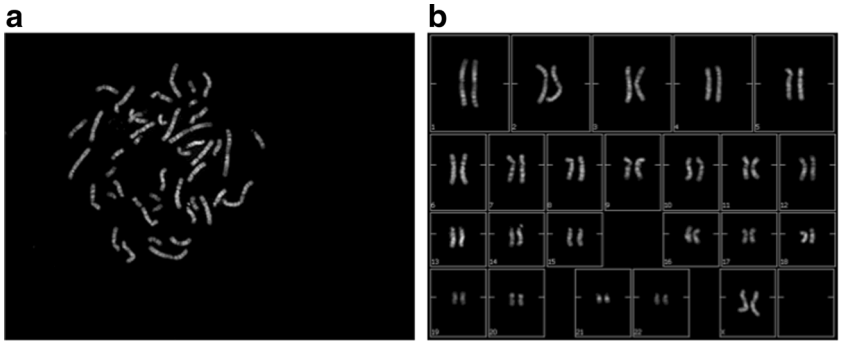

Fig. 4 Gene expression profile of osteogenic markers
Notes: Expression of osteogenic marker mRNAs in DPSCs seeded onto experimental implant compared to control implant at 15 and 30 days of culture. Data presented as the mean ± standard error of 3 measurements. * p value ≤0.05.

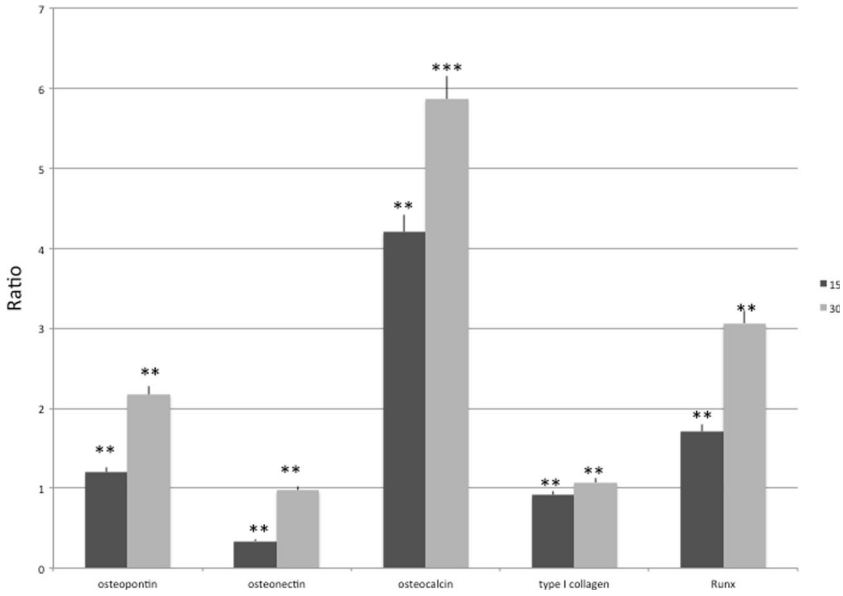

Fig. 5 IF staining of osteopontin
Notes: Osteopontin staining (red) in DPSCs seeded on experimental implant for 30 days. Nuclei (blue) are stained with Hoechst. (A) 5× magnification, (B) 10× magnification.

implants compared to those seeded onto the control ones. The presence of OPN at protein level has been evaluated trough IF staining (Fig. 5). From IF images it is clearly evident that the osteogenic marker OPN is expressed in all the cells seeded onto experimental implants.

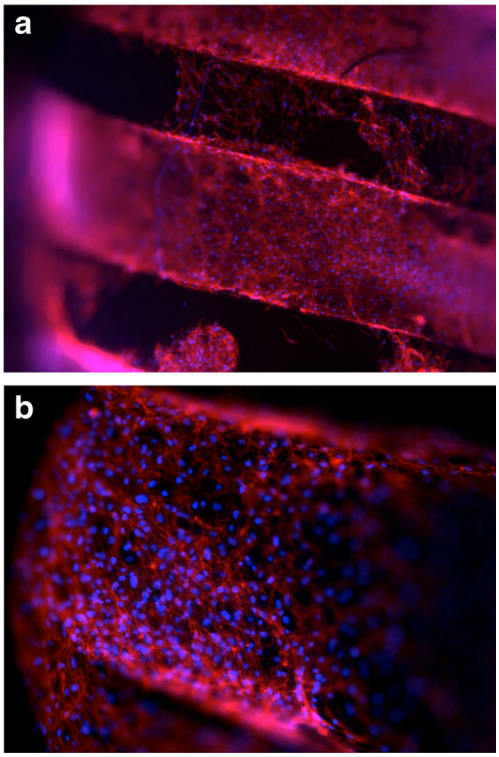

Fig. 6 ALP activity measurements
Notes: Intracellular and extracellular ALP activity were quantified in DPSCs cultured on experimental and control Ti implants for 30 days. * p value ≤0.05.

To further confirm the differentiation of DPSCs towards an osteoblast phenotype, the ALP activity was quantified both into cells and in culture medium. As shown in Fig. 6, the intracellular ALP activity was 0.543 U/mL for DPSCs grown on experimental implants and 0.341 U/mL for those seeded onto control implants. Even the extracellular ALP was higher in the experimental group (0.512 U/mL) in comparison to the control group, where it was slightly lower (0.324 U/mL).

A detailed analysis of surface markers involved in cell adhesion is reported in Fig. 7. There is not significant alteration in integrins (ITG) expression; on the contrary, a defined reduction in metalloproteinases (MMPs) and a significant increase of VCAM1, a protein related to an endothelial phenotype, occurs when cells were seeded on the experimental Ti implants.

Nowadays, miRNAs represent an important tool in biological and medical fields, due to their crucial role as biomarkers of several diseases. [34] In addition, recent studies have demonstrated the involvement of miRNAs in the osteogenic differentiation of stem cells. [35] It is well known that Mesenchymal Stem Cells (MSCs) possess both osteogenic and adipogenic differentiation potential, and that an inverse relationship between the two processes exists. Although different TFs that regulate adipogenic or osteogenic differentiation of MSCs have been described, the molecular mechanism at the basis of the MSCs commitment still remains to be elucidated. At the post-transcriptional level, miRNAs are known to influence both stability and protein expression of their mRNA targets; for this reason, these are now considered key regulators of several biological processes, including stem cell proliferation and differentiation. In the light of such considerations, in the last part of this work we have evaluated the expression of nine mature miRNAs known to influence

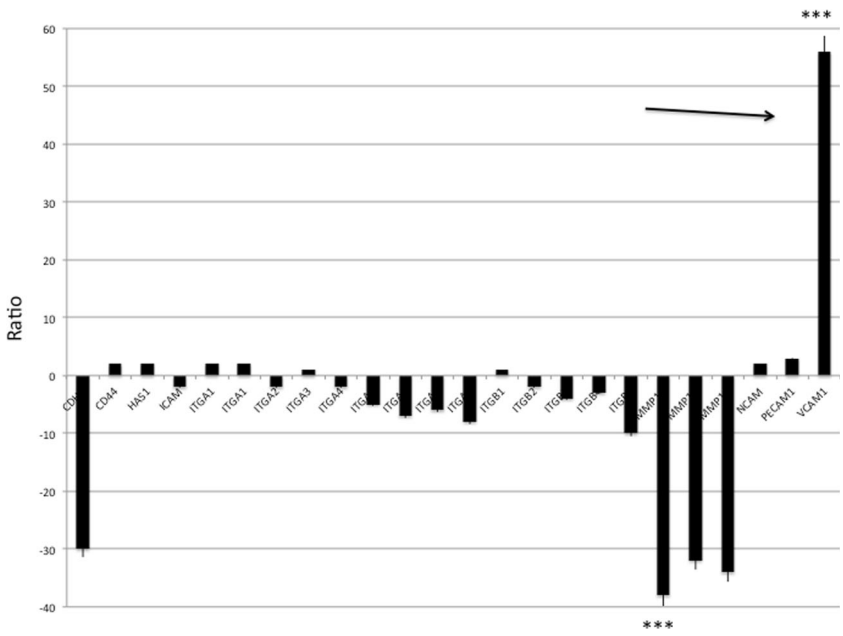

Fig. 7 Gene expression profile of cell adhesion surface markers
Notes: Expression of cell adhesion marker mRNAs in DPSCs seeded onto experimental implant compared to control implant at 30 days of culture. Data presented as the mean ± standard error of 3 measurements. * p value ≤0.05. Abbreviations: CDH1, cadherin 1; ITG, integrin; MMP, matrix metallopeptidase; ICAM1, intracellular adhesion molecule 1; NCAM1, neural cell adhesion molecule 1; PECAM1, platelet/endothelial cell adhesion molecule1; VCAM1, vascular cell adhesion molecule 1.

adipogenic and osteogenic differentiation of MSCs in opposite directions. As reported in Fig. 8, all the miRNAs involved into osteogenic differentiation of the stem cells are upregulated. Among these, miRNA-196a showed the highest upregulation. miR-196a exerts a fundamental role in the osteogenic commitment of MSCs, mainly through the modulation of Hox genes expression. [35] Hox genes code for a family of TFs with a relevant function in animals development. [36, 37] In particular, miR-196a seems to inhibit proliferation of MSCs and simultaneously enhance their osteogenic differentiation by binding to specific sequences in the 3′-UTR region of HOXC8 mRNA. In addition, miR-196a is found to be upregulated during osteogenic MSCs differentiation. Our results might corroborate these finding and confirm the role of miR-196a as a positive regulator of the osteogenic differentiation of DPSCs.

Conclusion

The effect of nanoscale modifications and coatings on Ti implant surfaces has recently received great attention in the field of biomaterial science. In the present study, the behavior of DPSCs seeded onto nanorough Ti surfaces treated with

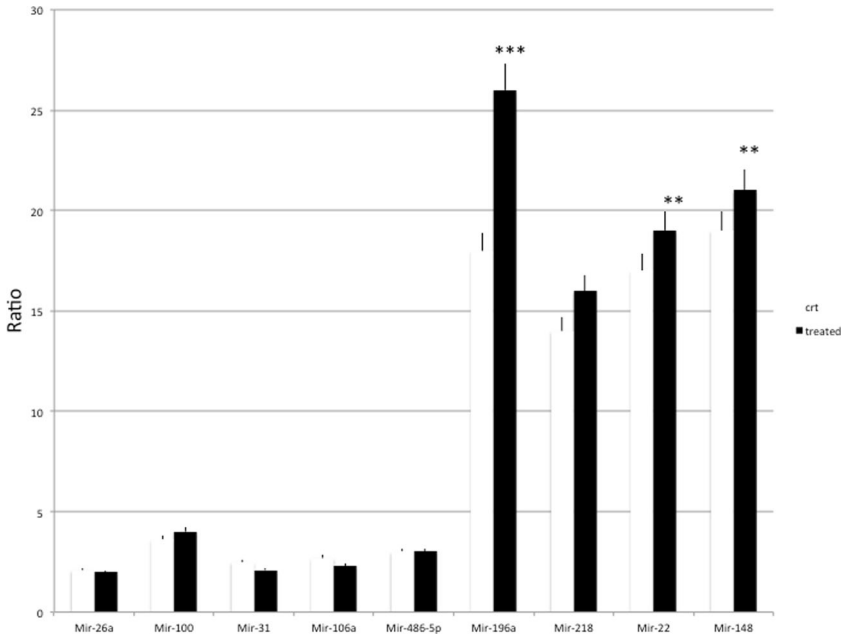

Fig. 8 Mature miRNAs expression profile
Notes: Expression profile of nine mature miRNAs in DPSCs cultured onto experimental and control Ti implants for 30 days. Data presented as the mean ± standard error of 3 measurements. * p value ≤0.05.

NWRBM has been evaluated and compared with that of AB/AE control surfaces. Enhanced osteogenic properties have been detected in cells grown onto the first type of implants, and this could probably be related to an increase in miRNA-196a and VCAM1 mRNA expression. The results of our study would confirm that the interactions between stem cells and implant surface are important regulators of cell commitment towards an osteogenic phenotype.

Author Contributions Conceived and designed the experiments: Barbara Zavan and Adriano Piattelli. Performed the experiments: Letizia Ferroni and Chiara Gardin. Analyzed the data: Letizia Ferroni, Chiara Gardin and Barbara Zavan. Contributed reagents/materials/analysis tools: Eitan Mijiritsky and Barbara Zavan. Wrote the paper: Chiara Gardin, Letizia Ferroni and Barbara Zavan.

Compliance with Ethical Standards

Disclosure The author reports no conflicts of interest in this work.

References

1. Ferraris, S., Vitale, A., Bertone, E., et al. (2016). Multifunctional commercially pure titanium for the improvement of bone integration: Multiscale topography, wettability, corrosion resistance and biological functionalization. *Materials Science & Engineering, C: Materials for Biological Applications, 60*, 384–393.
2. Mihailescu, N., Stan, G. E., Duta, L., et al. (2016). Structural, compositional, mechanical characterization and biological assessment of bovine-derived hydroxyapatite coatings reinforced with MgF2 or MgO for implants functionalization. *Materials Science & Engineering, C: Materials for Biological Applications, 59*, 863–874.
3. Cecchinato, D., Bressan, E. A., Toia, M., et al. (2012). Osseointegration in periodontitis susceptible individuals. *Clinical Oral Implants Research, 23*, 1–4.
4. Shemtov-Yona, K., & Rittel, D. (2015). An overview of the mechanical integrity of dental implants. *Biological Research International, 2015*, 547384.
5. Agarwal, R., & García, A. J. (2015). Biomaterial strategies for engineering implants for enhanced osseointegration and bone repair. *Advanced Drug Delivery Reviews, 94*, 53–62.
6. Rosa, V., Della Bona, A., Cavalcanti, B. N., et al. (2012). Tissue engineering: from research to dental clinics. *Dental Materials, 28*, 341–348.
7. Bressan, E., Carraro, A., Ferroni, L., et al. (2013). Nanotechnology to drive stem cell commitment. *Nanomedicine (London, England), 8*, 469–486.
8. Ferroni, L., Gardin, C., Della Puppa, A., et al. (2015). Novel nanotechnologies for brain cancer therapeutics and imaging. *Journal of Biomedical Nanotechnology, 11*, 1899–1912.
9. Bressan, E., Sbricoli, L., Guazzo, R., et al. (2013). Nanostructured surfaces of dental implants. *International Journal of Molecular Sciences, 14*, 1918–1931.
10. Kulkarni, M., Mazare, A., Gongadze, E., et al. (2015). Titanium nanostructures for biomedical applications. *Nanotechnology, 26*, 062002.
11. Zavan, B., Vindigni, V., Vezzù, K., et al. (2009). Hyaluronan based porous nano-particles enriched with growth factors for the treatment of ulcers: A placebo-controlled study. *Journal of Materials Science: Materials in Medicine*, 235–247.
12. Hao, J., Zhang, Y., Jing, D., et al. (2015). Mechanobiology of mesenchymal stem cells: perspective into mechanical induction of MSC fate. *Acta Biomaterialia, 20*, 1–9.
13. Wang, Y. K., & Chen, C. S. (2013). Cell adhesion and mechanical stimulation in the regulation of mesenchymal stem cell differentiation. *Journal of Cellular and Molecular Medicine, 17*, 823–832.
14. Yang, W., Han, W., He, W., et al. (2016). Surface topography of hydroxyapatite promotes osteogenic differentiation of human bone marrow mesenchymal stem cells. *Materials Science & Engineering, C: Materials for Biological Applications, 60*, 45–53.
15. Yang, C., Tibbitt, M. W., Basta, L., et al. (2014). Mechanical memory and dosing influence stem cell fate. *Nature Materials, 13*, 645–652.
16. Byun, M. R., Kim, A. R., Hwang, J. H., et al. (2014). FGF2 stimulates osteogenic differentiation through ERK induced TAZ expression. *Bone, 58*, 72–80.
17. Teo, B. K., Wong, S. T., Lim, C. K., et al. (2013). ACS nanotopography modulates mechanotransduction of stem cells and induces differentiation through focal adhesion kinase. *Nano, 7*, 4785–4798.
18. Gardin, C., Bressan, E., Ferroni, L., et al. (2012). In vitro concurrent endothelial and osteogenic commitment of adipose-derived stem cells and their genomical analyses through comparative genomic hybridization array: novel strategies to increase the successful engraftment of tissue-engineered bone grafts. *Stem Cells and Development, 21*, 767–777.
19. Becerra-Bayona, S., Guiza-Arguello, V., Qu, X., et al. (2012). Influence of select extracellular matrix proteins on mesenchymal stem cell osteogenic commitment in three-dimensional contexts. *Acta Biomaterialia, 8*, 4397–4404.
20. Quesenberry, P. J., Goldberg, L. R., & Dooner, M. S. (2015). Concise reviews: a stem cell apostasy: a tale of four H words. *Stem Cells, 33*, 15–20.
21. Maia, F. R., Bidarra, S. J., Granja, P. L., et al. (2013). Functionalization of biomaterials with small osteoinductive moieties. *Acta Biomaterialia, 9*, 8773–8789.
22. Earls, J. K., Jin, S., & Ye, K. (2013). Mechanobiology of human pluripotent stem cells. *Tissue Engineering. Part B, Reviews, 19*, 420–430.
23. Nava, M. M., Raimondi, M. T., & Pietrabissa, R. (2012). Controlling self-renewal and differentiation of stem cells via mechanical cues. *Journal of Biomedicine & Biotechnology, 2012*, 797410.
24. Bakhsheshi-Rad, H. R., Hamzah, E., Kasiri-Asgarani, M., et al. (2016). Deposition of nanostructured fluorine-doped hydroxyapatite-polycaprolactone duplex coating to enhance the mechanical properties and corrosion resistance of Mg alloy for biomedical applications. *Materials Science & Engineering, C: Materials for Biological Applications, 60*, 526–537.
25. Diez, M., Kang, M. H., Kim, S. M., et al. (2016). Hydroxyapatite (HA)/poly-L-lactic acid (PLLA) dual coating on magnesium alloy under deformation for biomedical applications. *Journal of Materials Science. Materials in Medicine, 27*, 34.
26. Lee JH, Jang HL, Lee KM, et al. Cold-spray coating of hydroxyapatite on a three-dimensional polyetheretherketone implant and its biocompatibility evaluated by in vitro and in vivo minipig model. *Journal of Biomedical Materials Research. Part B, Applied Biomaterials* 2015;

27. Miola, M., Verné, E., Ciraldo, F. E., et al. (2015). Electrophoretic deposition of chitosan/45S5 bioactive glass composite coatings doped with Zn and Sr. *Front Bioeng Biotechnol., 3*, 159.
28. Bonfante, E. A., Marin, C., Granato, R., et al. (2012). Histologic and biomechanical evaluation of alumina-blasted/acid-etched and resorbable blasting media surfaces. *The Journal of Oral Implantology, 38*, 549–557.
29. Gardin, C., Ferroni, L., Bressan, E., et al. (2014). Adult stem cells properties in terms of commitment, aging and biological safety of grit-blasted and acid-etched ti dental implants surfaces. *International Journal of Molecular Cell Medicine, 3*, 225–236.
30. Ferroni, L., Gardin, C., Bressan, E., et al. (2015). Ionized Ti surfaces increase cell adhesion properties of mesenchymal stem cells. *J Biomater Tissue Eng., 5*, 1–9.
31. Bressan, E., Ferroni, L., Gardin, C., et al. (2012). Donor age-related biological properties of human dental pulp stem cells change in nanostructured scaffolds. *PloS One, 7*, e49146.
32. Denizot, F., & Lang, R. (1986). Rapid colorimetric assay for cell growth and survival. Modifications to the tetrazolium dye procedure giving improved sensitivity and reliability. *Journal of Immunological Methods, 89*, 271–277.
33. Pfaffl, M. W. (2001). A new mathematical model for relative quantification in real-time RT-PCR. *Nucleic Acids Research, 29*, e45.
34. Deng, Y., Zhou, H., Zou, D., et al. (2013). The role of miR-31-modified adipose tissue-derived stem cells in repairing rat critical-sized calvarial defects. *Biomaterials, 34*, 6717–6728.
35. Kim, Y. J., Bae, S. W., Yu, S. S., et al. (2009). miR-196a regulates proliferation and osteogenic differentiation in mesenchymal stem cells derived from human adipose tissue. *Journal of Bone and Mineral Research, 24*, 816–825.
36. van Wijnen, A. J., van de Peppel, J., van Leeuwen, J. P., et al. (2013). MicroRNA functions in osteogenesis and dysfunctions in osteoporosis. *Current Osteoporosis Reports, 11*, 72–82.
37. Candini, O., Spano, C., Murgia, A., et al. (2015). Mesenchymal progenitors aging highlights a miR-196 switch targeting HOXB7 as master regulator of proliferation and osteogenesis. *Stem Cells, 33*, 939–950.